

# Multifractal scaling of the intrinsic permeability

Michel C. Boufadel

Department of Civil and Environmental Engineering, Temple University, Philadelphia, Pennsylvania

Silong Lu and Fred J. Molz

Environmental Engineering and Science Department, Clemson University, Clemson, South Carolina

Daniel Lavalley

Institute for Crustal Studies, University of California, Santa Barbara

**Abstract.** Existing fractal studies dealing with subsurface heterogeneity treat the logarithm of the permeability  $K$  as the variable of concern. We treat  $K$  as a multifractal and investigate its scaling and fractality using measured horizontal  $K$  data from two locations in the United States. The first data set was from a shoreline sandstone near Coalinga, California, and the second was from an eolian sandstone [Goggin, 1988]. By applying spectral analyses and computing the scaling of moments of various orders (using the double trace moment method [Lavalley, 1991; Lavalley et al., 1992]), we found that  $K$  is multiscaling (i.e., scaling and multifractal). We also found that the so-called universal multifractal (UM) [Schertzer and Lovejoy, 1987] model (essentially a log-Levy multifractal), was able to reproduce the multiscaling behavior reasonably well. The UM model has three parameters:  $\alpha$ ,  $\sigma$ , and  $H$ , representing the multifractality index, the codimension of the mean field, and the “distance” to stationary multifractal, respectively. We found ( $\alpha = 1.7$ ,  $\sigma = 0.23$ ,  $H = 0.22$ ) and ( $\alpha = 1.6$ ,  $\sigma = 0.11$ ,  $H = 0.075$ ) for the shoreline and eolian data sets, respectively. The fact that  $\alpha$  values were less than 2 indicates that the underlying statistics are non-Gaussian. We generated stationary and nonstationary multifractals and illustrated the role of the UM parameters on simulated fields. Studies that treated  $\text{Log } K$  as the variable of concern have pointed out the necessity for large data records, especially when the underlying distribution is Levy-stable. Our investigation revealed that even larger data records are required when treating  $K$  as a multifractal, because  $\text{Log } K$  is less intermittent (or irregular) than  $K$ .

## 1. Introduction

Field measurements of the intrinsic permeability  $K$  have shown that it is highly heterogeneous and that the bounds of heterogeneity increase as the scale of observation is increased [Molz and Boman, 1993]. The latter property is indicative of the statistical nonstationarity of  $K$ , which results in an apparent correlation length increasing with the scale of measurements. The combination of irregular, heterogeneous  $K$  and systematic increase of the irregularity with scale has led several researchers to apply fractal concepts [Mandelbrot, 1982] to  $\text{Log } K$  (throughout this work, “Log” and “log” refer to the natural logarithm and the logarithm base 10, respectively). Early monofractal models used in subsurface hydrology were the fractional Brownian motion (fBm) and the fractional Gaussian noise (fGn) models [Mandelbrot, 1982]. These models were adopted by various researchers [Hewett, 1986; Molz and Boman, 1993, 1995]. A more recent monofractal model is the fractional Levy motion (fLm) [e.g., Samorodnitsky and Taqqu, 1994], introduced to the field of subsurface hydrology by Painter and Paterson [1994] (see also Painter [1996] and Molz et al. [1997]). Recently, Liu and Molz [1997] treated  $\text{Log } K$  as a multifractal. They used for this purpose the so-called universal

multifractal [Schertzer and Lovejoy, 1987] model (essentially a log-Levy multifractal).

All of these approaches treated  $\text{Log } K$  as the variable of concern. So the actual  $K$  distribution is an exponentiated monofractal or an exponentiated multifractal. Exponentiated Levy monofractals and the exponentiated multifractal obtained by Liu and Molz [1997] produce fields having no finite theoretical statistical moments. Painter [1998] developed a bounded fLm model that allows the existence of finite low-order statistical moments upon exponentiation, and recently, Painter and Mahinthakumar [1999] conducted numerical experiments and found that a bounded fBm or fLm model of  $\text{Log } K$  results in essentially a multifractal  $\text{Log } K$ .

In our opinion, there is no obvious reason to treat  $K$  through the “window” of the logarithm, and we propose to treat it directly as a multifractal. We analyze for this purpose intrinsic permeability data from two fields in the United States and test the multifractality of  $K$ . We also estimate the parameters of the so-called universal multifractal (UM) model developed by Schertzer and Lovejoy [1987] and use the estimated parameters to generate synthetic multifractal fields.

## 2. Multifractals

Multifractals is a relatively new mathematics introduced in the 1980s to study strange attractors [Hentschel and Procaccia, 1983; Halsey et al., 1986] and the spatial distribution of the

Copyright 2000 by the American Geophysical Union.

Paper number 2000WR900208.  
0043-1397/00/2000WR900208\$09.00

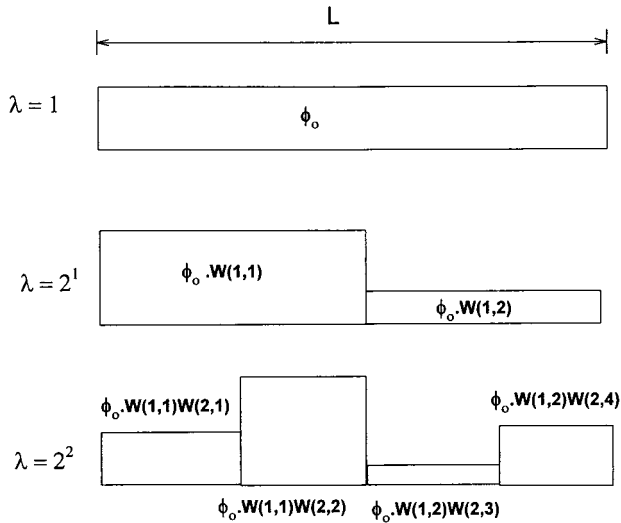


**Figure 1.** Schematic of a multiplicative cascade. The ensemble average of  $\phi$  is conserved at any level. As one proceeds down the cascade, the field becomes more intermittent.

kinetic energy dissipation rate in fully developed turbulence [Frisch and Parisi, 1985]. Following existing works in geophysics, we will borrow from the latter situation in presenting multifractals and applying them to  $K$  fields.

Kolmogorov [1949, 1962], Obukhov [1962], and Yaglom [1966] had established that in fully developed turbulence, large-scale eddies transmit their kinetic energy without dissipation to smaller-scale eddies, which in turn transmit their energy (without dissipation) to smaller-scale eddies, down to the Kolmogorov scale, where energy is dissipated by viscosity. This process has been represented mathematically with a multiplicative cascade, which, to date, appears to be the only mechanisms for generating a stationary multifractal field.

Figure 1 illustrates the construction of a three-level multiplicative cascade in a one-dimensional space. Consider the field  $\phi_0$  at step 0 distributed uniformly over the length  $L$ , divide  $L$  in  $b$  segments ( $b = 2$  in Figure 1, but any other integer value  $>2$  could be used), generate  $b$  positive random variables  $W_{i,j}$  ( $i = 1, j = 1, b$ ) (the probability distribution of the weights is discussed below), and multiply each one of them by the field in a corresponding segment selected randomly. Repeat at level 2 the procedure conducted at level 1 using  $b^2$  weights. Hence the field  $\phi_i$  is random for  $i > 1$ , and the scale ratio  $\lambda = b^i$  increases with each cascade step  $i$ . The weights have to be selected such that their average is equal to 1 at each cascade level to conserve the average value of the field at each level. When the cascade is iterated indefinitely ( $\lambda$  tends to infinity), the resulting field  $\phi$  is a statistical multifractal (as opposed to a deterministic multifractal). However, from a practical point of view, it suffices that the scale ratio becomes sufficiently large (say,  $i > 7$ ) to obtain an essentially multifractal field (see, for example, the work of Meneveau and Sreenivasan [1987a]).

If one requires conservation of the ensemble average of the field at each cascade level  $\langle W \rangle = 1$  (where angle brackets designate ensemble average), then a so-called canonical multifractal field is obtained [Mandelbrot, 1974]. This is the case of interest to us because it is more general than the case where conservation of the average is enforced over each realization,

which results in a microcanonical multifractal field; an example of such a field is the binomial “ $p$  model” [Meneveau and Sreenivasan, 1987b]. A thorough discussion of the classification of multifractals is given by Schertzer *et al.* [1991] and Gupta and Waymire [1993]. It is worth mentioning that although the weights are independent, the field itself is correlated due to the construction procedure.

### 2.1. Probability Distribution of the Weights

Going back to the multiplicative cascade and setting  $\phi_0 = 1$  for convenience, the field at cell  $j$  after  $i$  cascade steps is given by

$$\phi(i, j) = W_1 \times W_2 \times \cdots \times W_i, \quad (1)$$

where the spatial dependence of the weights at steps  $< i$  are omitted for simplicity. Taking the logarithm on both sides of (1) results in

$$\text{Log } \phi(i, j) = \text{Log } W_1 + \text{Log } W_2$$

$$+ \text{Log } W_3 + \cdots + \text{Log } W_i. \quad (2)$$

If one uses weights  $W$  that are independent and drawn from the same distribution that has a finite variance, the central limit theorem (CLT) applied to (2) results in  $\text{Log } \phi(i, j)$  following a normal distribution (the weights  $W$  have to be properly normalized). Thus  $\phi(i, j)$  follows a lognormal distribution. This is the model introduced by Kolmogorov [1962], Obukhov [1962], and Yaglom [1966]. However, with the emergence of fractals and scaling, Mandelbrot [1974] argued that the lognormal model can only be obtained “under extreme and unlikely conditions” and proposed weights belonging to a distribution with an infinite variance. (The tail of the probability density function (pdf) of such distributions follows a power law and hence drops at a much slower rate than that of the Gaussian distribution. Such distributions are also termed fat tailed or heavy tailed [Waymire, 1985].) Later, Gupta and Waymire [1991] showed that a multifractal field obtained from the lognormal model is scaling in at most a second-order sense (i.e., moments with order greater than 2 are not scaling).

A generalization of the lognormal model was introduced by Schertzer and Lovejoy [1987] and independently by Brax and Peschanski [1991] and Kida [1991]; it includes situations where the variance of  $W$  is infinite. In such a case, the generalized central limit theorem (GCLT) [Feller, 1971, p. 258] results in  $\text{Log } \phi(i, j)$  following a Levy-stable probability distribution. Note that the weights  $W$  do not have to be Levy; they could belong to any distribution that has a power law type tail. A family of such distributions is the Pareto [Mandelbrot, 1982]. Schertzer and Lovejoy [1987] termed their model universal multifractal (UM). However, as a comprehensive understanding of multifractals emerges, such terminology may turn out to be an overstatement [Gupta and Waymire, 1990; Veneziano, 1999]. Nevertheless, the UM model appears to be a general model, and we will use it in this work.

The Levy distribution (Figure 2) depends on four parameters:  $\alpha$ ,  $\beta$ ,  $\mu$ , and  $\sigma$ . Thus one can express a Levy noise  $S$  as  $S(\alpha, \beta, \mu, \sigma)$ . The parameter  $\alpha$  is such that  $0 < \alpha \leq 2$ , where the situation  $\alpha = 2$  corresponds to the Gaussian distribution (Figure 2). The statistical moments of order  $m$  are not defined for  $m \geq \alpha$ , with the exception of the Gaussian case where all statistical moments are defined. Thus the variance is infinite for  $\alpha < 2$ , and the mean is infinite for  $\alpha < 1$ . The parameter

$\mu$  is a real number and is a centering term. It is equal to the mean of the distribution only when  $\alpha > 1.0$  and  $\beta = 0$ . The parameter  $\mu$  is usually set to zero in monofractal applications [Painter, 1996; Molz et al., 1997] and multifractal applications [Schertzer and Lovejoy, 1987]. The parameter  $\beta \in [-1; 1]$  is known as the skewness parameter:  $\beta = -1$  gives an extreme negative antisymmetric distribution, where the probability of producing negatively large random variables is high, the converse occurs for  $\beta = 1$ , and  $\beta = 0$  results in a symmetric distribution with respect to  $\mu$ . Note that the antisymmetric situation where all values are of one sign (negative for  $\beta = -1$ , positive for  $\beta = 1$ ) occurs only for  $0 < \alpha < 1$  [Samorodnitsky and Taqqu, 1994]. The parameter  $\beta$  is irrelevant whenever  $\alpha = 2$  and is set equal to zero in Levy monofractal applications [Painter, 1996; Liu and Molz, 1997] and to  $-1$  in multifractal applications [Schertzer and Lovejoy, 1989]. The situation  $\beta = -1$  is required to ensure that low-order statistical moments of  $\phi$  exist [Schertzer and Lovejoy, 1987; Gupta and Waymire, 1993]. The parameter  $\sigma$  is known as the scale parameter; it is equal to half the variance in the case  $\alpha = 2$  and plays a similar role when  $\alpha < 2$  (i.e., it is a measure of the width of the distribution (Figure 2)).

## 2.2. Properties of Multifractal Fields

Considering a multifractal field  $\phi_\lambda$  at a scale ratio  $\lambda$ , one can write [Schertzer and Lovejoy, 1987; Frisch, 1996]

$$\Pr(\phi_\lambda \geq \lambda^\gamma) \sim \lambda^{-C(\gamma)}, \quad (3)$$

where Pr stands for “probability” and the tilde means equality within slowly varying constants (such as logarithm of  $C(\gamma)$ ). Here  $\gamma$  is a real variable termed the “order of singularity.”  $C(\gamma)$  is known as the codimension of the field and is a non-linear increasing and concave (facing upward) function of  $\gamma$ . For a fixed  $\lambda$ , (3) states a well-known fact: If one sets a threshold  $\lambda^\gamma$ , the probability of finding values of the field that exceed the threshold decreases with an increase in  $\gamma$  (because  $C(\gamma)$  is an increasing function of  $\gamma$ ). However, and more important, (3) states that the probability distribution of the field scales based solely on the scale ratio (i.e., there is no characteristic scale). Because  $C(\gamma)$  varies with  $\gamma$ , the exceedance probability at each threshold value scales differently than another value. This is known as multiscaling. The monoscaling case occurs when  $C(\gamma)$  is constant, which corresponds to a monofractal field.

Rather than specify the statistical properties via the multiple scaling of the probabilities (equation (3)), one can, equivalently, specify the multiple scaling of the moments:

$$\langle \phi_\lambda^q \rangle \sim \lambda^{M(q)}, \quad (4)$$

where  $\phi_\lambda^q$  is the  $q$ th moment of the field, the angle brackets represent ensemble averages, and  $M(q) \in \mathbb{R}$  is an exponent related to  $C(\gamma)$  by the Legendre transform when  $\lambda \rightarrow \infty$  [Frisch and Parisi, 1985]:

$$M(q) = \max_\gamma [q\gamma - C(\gamma)] \quad (5a)$$

$$C(\gamma) = \max_q [q\gamma - M(q)]. \quad (5b)$$

Equations (5) establish a one-to-one correspondence between the order of singularity and the moment order. A field is multifractal if  $M(q)$  is a concave (upward looking) nonlinear function of  $q$ .  $M(q) = 0$  for an additive monofractal field,

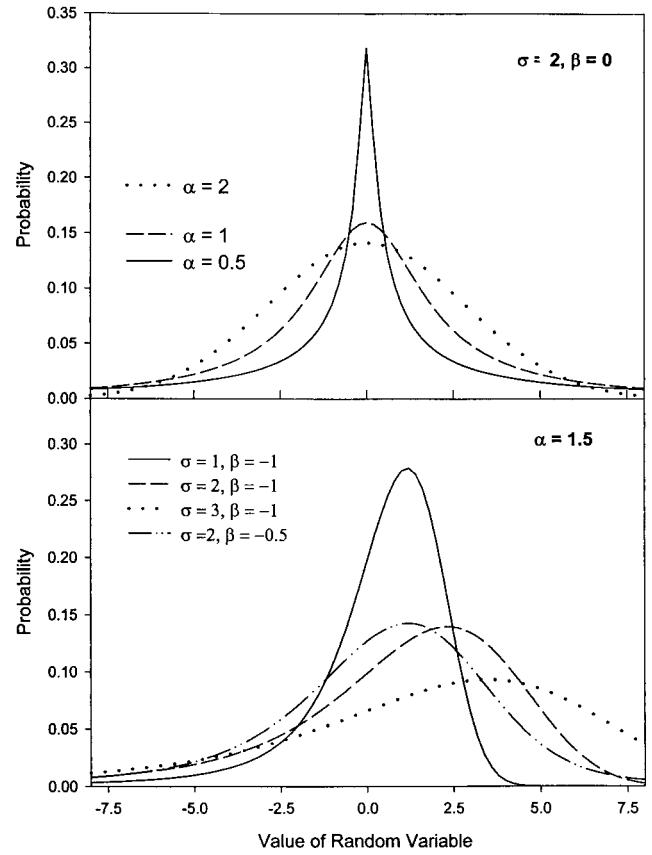


**Figure 2.** Probability density functions of Levy distributions;  $\alpha = 2$  corresponds to the Gaussian case.

such as an fBm [Molz and Boman, 1993], and  $M(q)$  is a linear function of  $q$  for a multiplicative monofractal field, such as the so-called  $\beta$  model [Mandelbrot, 1974; Frisch et al., 1978]. (The  $\beta$  in “ $\beta$  model” is not related to that of the Levy distribution.) When the field  $\phi_\lambda$  is a UM [Schertzer and Lovejoy, 1987],

$$M(q) = \frac{\sigma}{(\alpha - 1)} [q^\alpha - q]. \quad (6)$$

In the UM framework the term  $\sigma$  represents also the codimension of the mean field and  $\alpha$  represents the degree of multifractality:  $\alpha = 2$  represents a lognormal multifractal model, while  $\alpha = 0^+$  represents the (multiplicative) monofractal  $\beta$  model.

The field  $\phi$  is stationary, and its power spectrum has the form [Monin and Yaglom, 1975; Meneveau and Sreenivasan, 1987a]

$$E_\phi \propto k^{-[1-M(2)]}, \quad (7)$$

where the equality sign implies proportionality and  $k$  is the wave number in Fourier space. Equation (7) shows that the spectrum is a power law type with a spectral slope (the slope of  $\log E$  versus  $\log k$ ) less steep than a  $1/f$  noise (because  $M(2) > 0$ ). However, many geophysical fields, such as the hydraulic conductivity field, have spectral slopes that are different from  $-[1 - M(2)]$ , most commonly smaller than  $-[1 - M(2)]$  (i.e., the curve is steeper). Such fields are typically nonstationary fields and are discussed below.

### 2.3. Nonstationary Multifractals

A generic equation for dealing with geophysical fields (e.g., the intrinsic permeability) is [Schertzer and Lovejoy, 1987; Davis et al., 1994a, 1994b, 1996]

$$\Delta Q_\lambda \doteq \phi_\lambda \lambda^{-H}, \quad (8)$$

where the equality symbol implies equality in probability distribution ( $a \doteq b$  is equivalent to  $\Pr(a > p) = \Pr(b > p)$  for all  $p$ ).  $\Delta Q_\lambda$  are the “increments” of  $Q_\lambda$ , and  $H$  is an empirical coefficient obtained experimentally. Equation (8) shows that  $Q_\lambda$  can only be obtained from the field  $\phi_\lambda$  by a fractional integration of order  $H$  [Lovejoy et al., 1995], and hence  $\Delta Q_\lambda$  are not ordinary increments for  $H \neq 0$ . Fractional integration requires a convolution in the physical space [Tatom, 1995] but can be easily achieved in Fourier space simply by multiplying the Fourier transform of the field  $\phi_\lambda$  by  $k^{-H}$ , where  $k$  is the wave number [Lovejoy et al., 1995]. For  $H = 0$ ,  $\Delta Q_\lambda$  is an ordinary increment, and  $Q_\lambda$ , which in this case is a stationary multifractal, can be obtained from  $\phi_\lambda$  by standard integration, resulting in  $Q_\lambda = r\phi_\lambda + s$ , where  $r$  and  $s$  are constants selected to present  $Q_\lambda$  in the appropriate range depending on the units.

Equation (8) emerged in the area of turbulence, where  $Q$  represented the velocity and  $\phi$  represented the kinetic energy flux from large scales to smaller scales. The exponent  $a$  was found by dimensional arguments to be  $a = 1/3$  [Kolmogorov, 1949],  $H$  was also measured to be  $1/3$ . Equation (8) or equivalent forms of it have been used to study many geophysical fields such as water in the atmosphere [Schertzer and Lovejoy, 1987; Davis et al., 1996], river flows [Gupta and Waymire, 1990], land topography [Lavalley, 1991; Lavalley et al., 1993; Lovejoy et al., 1995], and ice deposition [Schmitt et al., 1995]. In all cases the parameter  $a$  was set equal to 1 and  $H$  was estimated based on the data. By substituting  $K$  for  $Q$  in (8), the spectrum of  $K$  is [Schertzer and Lovejoy, 1987; Davis et al., 1994a, 1996]

$$E_K \propto k^{-T}, \quad (9)$$

where  $T = 2H + 1 - M(2)$ . By comparing (7) with (9), one notes that the term  $2H$  appears in the exponent of the latter. It has been argued [Schertzer and Lovejoy, 1987; Lovejoy et al., 1995; Davis et al., 1994a, 1994b, 1996] that the field ( $Q$  or  $K$ ) is stationary for  $T < 1$  and nonstationary for  $T > 1$ . However, as acknowledged in some of these works [Davis et al., 1994a, 1994b, 1996], a rigorous fundamental proof for stationarity for  $T < 1$  has not been established. For this reason, we consider that multifractal fields are nonstationary whenever  $H > 0$  even if  $T < 1$ .

### 3. Method of Analysis

In this work we proceed as follows: Having an intrinsic permeability data field, (1) we plot  $\log E_K$  as a function of  $\log k$ . If the plot can be well approximated by a straight line (equation (9)), then the field is scaling. This step is a necessary condition for the field to be multifractal but is not a sufficient one (i.e., the field may be monofractal). (2) We take the absolute values of the increments of the field, thus creating a new field  $F$ . (Note that the field  $F$  is not necessarily equal to the field  $\phi$ .) (3) If (4) is satisfied (i.e., the function  $M(q)$  is nonlinear in  $q$ ), then the fields  $F$  and  $K$  are multifractal. (4) We estimate the parameters of the UM model ( $\alpha$ ,  $\sigma$ , and  $H$ ) based on  $K$  data (discussed below), and (5) we use the UM model to

generate synthetic multifractal fields. In step 4 we use the double trace moment (DTM) method [Lavalley, 1991; Lavalley et al., 1992] to estimate  $\alpha$  and  $\sigma$ , and then we factor them into (6) and compute  $M(2)$  to find  $H = [T - 1 + M(2)]/2$  from (9). The DTM method was designed to estimate  $\alpha$  and  $\sigma$ , but it could also be used to assess the nonlinearity of  $M(q)$  independent of the UM model assumption.

Consider a stationary multifractal field  $F$  at fine resolution  $\lambda'$  (Figure 3, where for simplicity  $L = 1$ ). The local average of  $F_\lambda$ , raised to the power  $\eta$  over an observing set  $B_\lambda$  with  $\lambda < \lambda'$ , is given by the following expression:

$$\Omega_\lambda(B_\lambda) = \frac{\int_{B_\lambda} F_\lambda^\eta d^D x}{\int_{B_\lambda} d^D x}, \quad (10)$$

where  $D$  is the dimension of the embedding space and  $d^D x$  implies a  $D$ -dimensional differential volume. For example,  $d^2 x = dx_1 \times dx_2$ , where  $x_1$  and  $x_2$  are two orthogonal directions in the plane. The  $q$ th-order DTM is obtained by computing the average value of the dressed moments raised to the power  $q$ . The scaling of the  $q$ th-order DTM is as follows:

$$\text{DTM}_q = \left\langle \sum_i [\Omega_\lambda(B_{\lambda_i})]^q \right\rangle \propto \lambda^{M(q,\eta)}. \quad (11)$$

The summation should be done on all disjoint sets (i.e., non-intersecting sets or intervals). The exponent  $M(q, \eta)$  is equal to  $M(\eta q) - qM(\eta)$ , which implies that  $M(q, 1) = M(q)$ , because  $M(1) = 0$  due to conservation of the average. Hence, when  $\eta = 1$ , (11) reduces to (4), and the DTM method in this special case allows assessment of the multifractality of a field without recourse to any multifractal model.

When the UM model is used, the following equation results [Lavalley, 1991; Lavalley et al., 1992, 1993]:

$$M(q, \eta) = \eta^\alpha M(q). \quad (12)$$

Therefore  $\alpha$  can be estimated on a simple plot of  $\log |M(q, \eta)|$  versus  $\log \eta$  for fixed  $q$  values. The observed intercept (for  $\eta = 1$ ) gives the value of  $\log |M(q, 1)| = \log |M(q)|$ . Once  $M(q)$  and  $\alpha$  are known,  $\sigma$  can be obtained from (6). The DTM method allows accurate estimation of  $\alpha$  and  $\sigma$  because one can use many  $\eta$  values around the mean of the field. Estimation of  $\alpha$  and  $\sigma$  using the (single) trace moments (i.e., for  $\eta = 1$ ) entails a poor nonlinear regression, especially at relatively large  $q$  values [Lavalley, 1991; Schertzer et al., 1991; Lavalley et al., 1992, 1993].

### 4. Data Analyses

We utilized  $K$  data obtained from two different geographical locations in the United States. The first data set is from an oil field in a shoreline sandstone near Coalinga, California. The second data set is from an eolian sandstone in northern Arizona [Goggin, 1988]. Both data sets were obtained by air permeameter on cores extracted from the soil.

The data from Coalinga were obtained from five well-cores. The vertical spacing of measurements was 0.3048 m (1 foot). Owing to missing measurements, we were able to utilize only portions of the data. The selected data set consisted of six

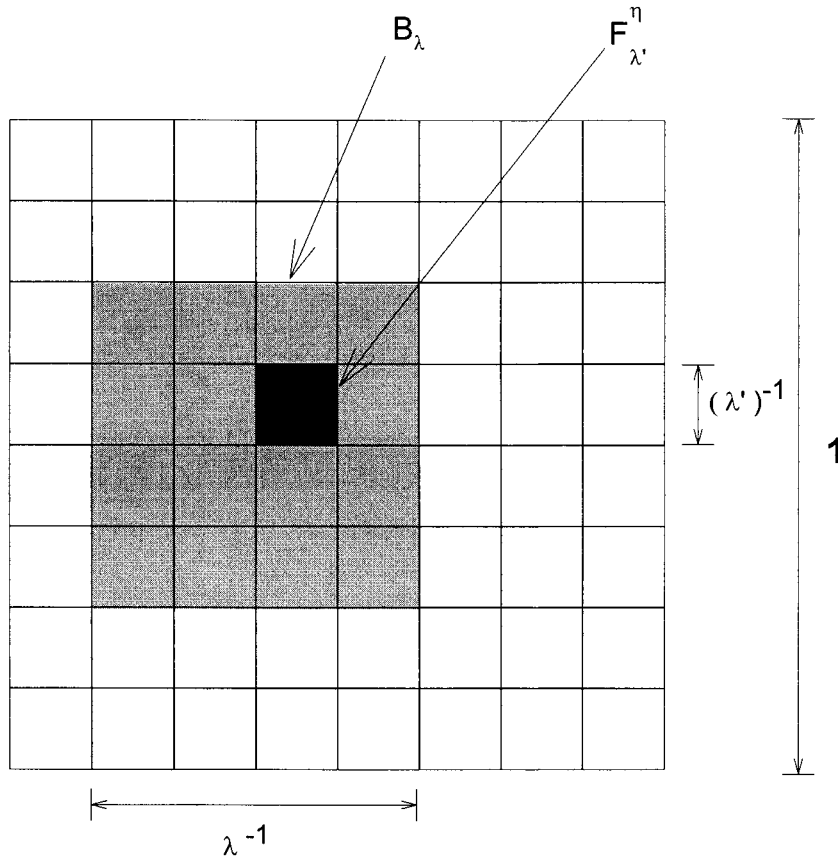


**Figure 3.** The double trace moment method. The field  $F$  is transformed to a field  $F^\eta$ , and moments of order  $q$  are averaged over arbitrary sets  $B_\lambda$ .

subsets, each containing 32 measurements (a total of 196 data points).

For the data from *Goggin* [1988] we used two transects and treated them as having identical statistical properties. We further reduced the data to obtain 36 data subsets (18 from each transect), each containing 64 data points (a total of 2304 data points). The spacing was 0.0125 m, but some of the subsets contained up to two separate spacings, each equal to 0.025 m. We substituted for the missing data by interpolating between neighboring nodes using the geometric average. Owing to the small number of missing data (a total of seven data points in the whole data set), this does not affect the outcome of the analyses. Implicit in the approach pursued here is that the statistical properties of the horizontal permeability do not vary with depth. This assumption will be reevaluated in future works.

Figures 4 and 5 show permeability measurements from Coalinga and *Goggin* [1988], respectively. CO1A and CO1B represent a continuous record, and so do CO2A and CO2B. Although splitting records in half reduces the range of scaling, it provides more stable results due to the averaging over a higher number of data sets. This approach was adopted by *Meneveau and Sreenivasan* [1987a] in analyzing velocity fluctuations in turbulent flows.

Figures 4 and 5 both show the intermittent nature of the intrinsic permeability, where sudden large increases are noted. Although one tends to say that, for example, CO1A is more intermittent than CO2A, one has to note that the low values in CO2A are much smaller than those of CO1A, resulting in a

larger order of magnitude of fluctuations. Further discussion on intermittency in geophysical fields can be found elsewhere [*Davis et al.*, 1994a, 1996].

#### 4.1. The Spectrum

We computed the average spectrum for each data set by averaging the spectrum over the corresponding subsets. The results are reported in Figure 6, where  $\log E_K$  is plotted as a function of  $\log f$ , where  $f$  is the frequency,  $f = k/(N\Delta)$ ,  $N$  is the number of data points, and  $\Delta$  is the spatial increment. The range of  $f$  values is from  $1/(N\Delta)$  to  $1/2$ , the upper limit being the Nyquist frequency [*Peißen and Saupe*, 1988]. Figure 6 shows that a clear scaling is present over the whole range (with the exception of the shortest wave length of Coalinga, which was not used in the fitting), as evidenced by the high  $R^2$  values. Some of the wavelengths ( $f^{-1}$ ) are reported at the bottom of the panels, and they correspond to  $\log f$  above them on the abscissa axis. The results of Figure 6 are to our knowledge, the first time that scaling of  $K$  is investigated in the scientific literature. As discussed in section 1, existing studies investigated the scaling of  $\text{Log } K$ .

#### 4.2. Multifractality of $K$

To assess the multifractality of  $K$ , we applied the DTM method on the field  $F$  (i.e., the absolute value of the increments of  $K$ ) with  $\eta = 1$  for 41 values of  $q$  ranging from 0 to 4.0 at an increment of 0.1. Figures 7 and 8 show plots of  $\log \text{DTM}_q$  as a function of  $\log \lambda$  for selected values of  $q$ : The slope of the best fit straight line gives the value of  $M(q)$ . Both figures show

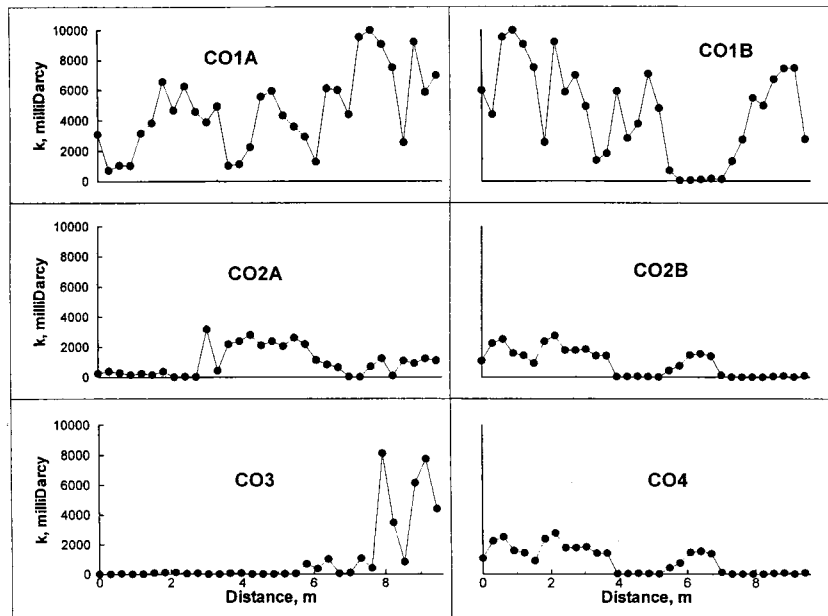


Figure 4. Permeability measurements from Coalinga as a function of depth.

that a linear relation (i.e., scaling) does not occur over the whole range of  $\lambda$  at low  $q$  values and that the range of linear relation increases with increasing  $q$  values. We attribute this behavior to the presence of noise in the data and the finiteness of the number of the data sets. When low-order moments ( $q < 1$ ) are computed, the contribution of the small values of the field to the ensemble average (equation (4)) is increased, while the contribution of the large values of the field is reduced. If the experimental errors are due to noise, then the contribution of the noise will mainly affect the small values of the field, since they are of the same order of magnitude. Hence the effect of noise in data is more important for  $q < 1$ . This problem is less severe if more subsets are considered. We investigated this behavior by considering nine and 18 subsets of

Goggin [1988] instead of the 36 subsets used in Figure 8, and we observed that the scaling was less clear going from 36 to nine subsets (not shown). The fact that scaling is more apparent for a large number of short-range sets in comparison with a small number of long-range sets has been reported by *Meneveau and Sreenivasan* [1987a] in dealing with velocity fluctuations in turbulent flows.

We computed  $M(q)$  values by fitting straight lines to the portion of the graphs where a linear trend can be assumed. For the Coalinga data the first two points were discarded for  $q < 1$  (upper panel of Figure 7), and the last point was discarded for  $q > 1$  (lower panel of Figure 7). For Goggin's data the first two points and the last point in the upper panel of Figure 8 ( $q < 1$ ) were discarded, and the first point in the lower panel

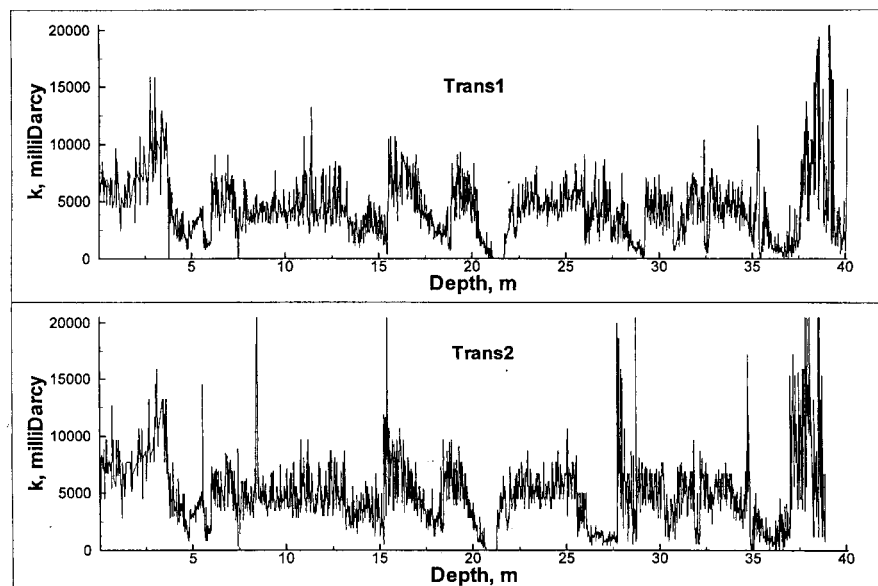


Figure 5. Permeability measurements from Goggin for transects 1 and 2 as a function of depth.

of Figure 8 ( $q > 1$ ) was discarded. This procedure was applied to all the values of  $q$  used (i.e., not only to those reported in Figures 7 and 8).

Figure 9 shows plots of the experimental  $M(q)$  as function of  $q$  for Coalinga and Goggin (circles). The theoretical curves obtained from the UM model are also reported and are discussed later in this paper. The Coalinga curve exhibits a nonlinear behavior for  $q$  less than 1.2 and a linear behavior for  $q > 1.2$ , while  $M(q)$  for the Goggin data appears to be nonlinear concave for about  $q < 3$  and linear for  $q > 3$ . Because of the nonlinear behavior, we conclude that the intrinsic permeability for both Coalinga and Goggin data is multifractal.

The change from nonlinear to linear behavior at a certain  $q$  value is due to undersampling and is typical of multifractal fields of finite length [Lavalley, 1991; Lavalley et al., 1993]. The larger the order  $q$  of the statistical moments is, the more they are dominated by extreme events, which, by definition, are poorly sampled in data analysis situations [Lavalley, 1991; Lavalley et al., 1993; Davis et al., 1994b]. Evidently, the  $q$  value at which the change in behavior occurs depends also on the length of the data record under consideration, with longer records permitting higher  $q$  values.

As found below, the Coalinga  $K$  field is more intermittent than that of Goggin, and only 198 data points were used from Coalinga, in comparison with 2304 data points from Goggin field. Hence the fact that the change of behavior from nonlinear to linear for Coalinga occurred at a low  $q$  value ( $q = 1.2$ )

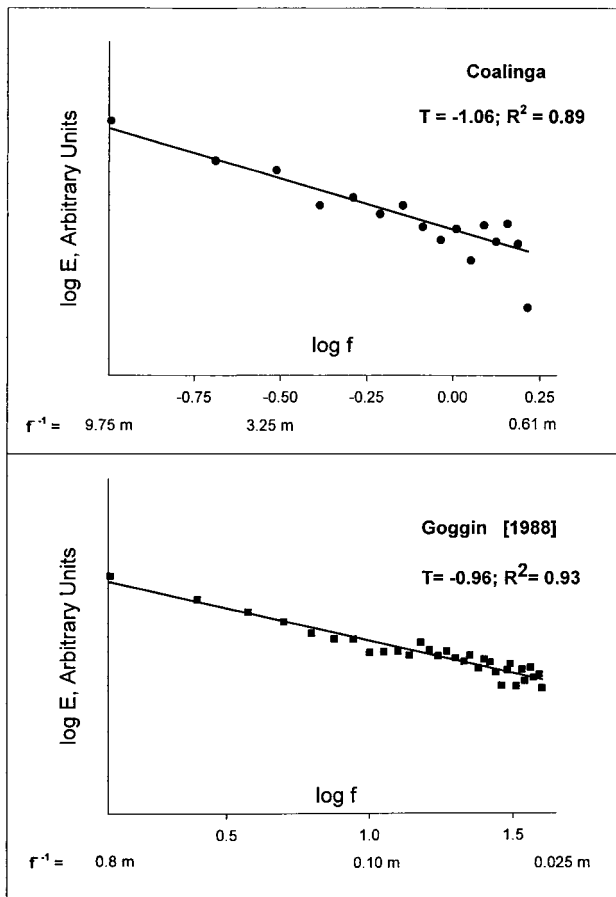


**Figure 6.** Spectra of Coalinga and Goggin. The high  $R^2$  values indicate that the permeability is scaling.

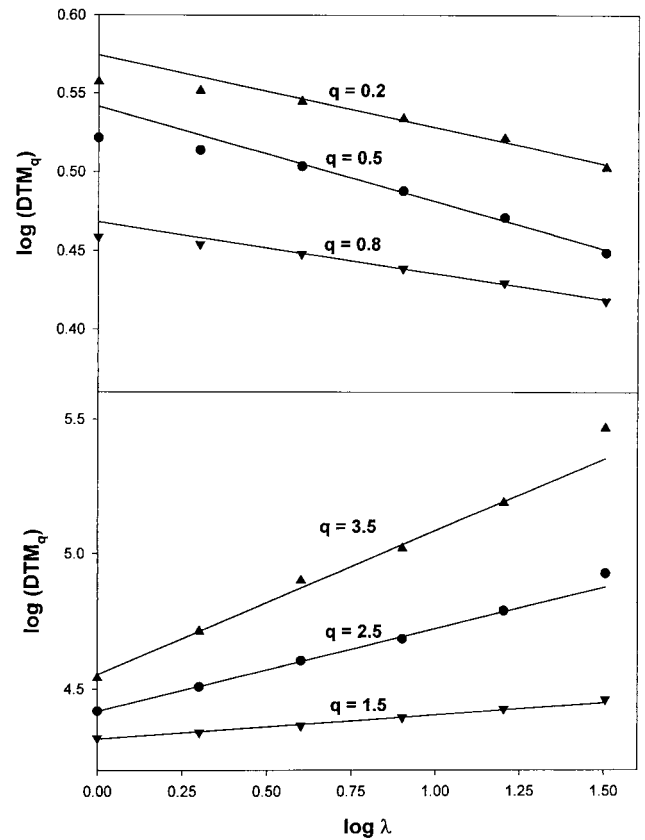


**Figure 7.** Scaling of the moments for various values of  $q$  for the Coalinga field. The first two points of the top panel and the last point of the bottom panel were not used in fitting straight lines to data.

in comparison with that of Goggin ( $q = 3.0$ ) is understandable.

#### 4.3. The Permeability $K$ as a Universal Multifractal

For the Coalinga data set the DTM method was applied on the field  $F$  for  $q = 0.5$  and  $1.5$  (equations (10) and (11)) and for 20  $\eta$  values ranging from 0.1 to 2.0 (at a constant logarithmic increment). For the Goggin data set the DTM method was applied on the field  $F$  for  $q = 1.2$  and  $1.8$  and for 20  $\eta$  values ranging from 1.1 to 2.6 (at a constant logarithmic increment). High  $q$  values for the Goggin data were adopted because of the limited range of scaling at small values of  $\max(q, q\eta)$  (note Figure 8 for  $\eta = 1$ ). Figures 10 and 11 show the scaling of the  $DTM_q$  for Coalinga and Goggin, respectively. The slope of the best fit straight lines gives the values of  $M(q, \eta)$ . The first data point in Figure 11 was not used in fitting the straight lines.

Plots of  $\log |M(q, \eta)|$  as function of  $\log \eta$  are reported in Figure 12. Undersampling causes  $\log |M(q, \eta)|$  to reach a plateau at high  $q$  values. Straight lines are fitted to the linear part of the curves. For each  $q$  value the slope of the curve gives the value of  $\alpha$  and the intercept provides  $\sigma$  (section 3.1). The estimated values of  $\alpha$  and  $\sigma$  are reported in Table 1, which shows that the estimates at different  $q$  values are close. Also reported are the arithmetic averages of  $\alpha$  and  $\sigma$  for the  $q$  values used. Note that  $\alpha < 2$ , which implies that the underlying statistics are non-Gaussian.

The difference in  $\alpha$  between Coalinga and Goggin data is not significant from a practical point of view (based on our

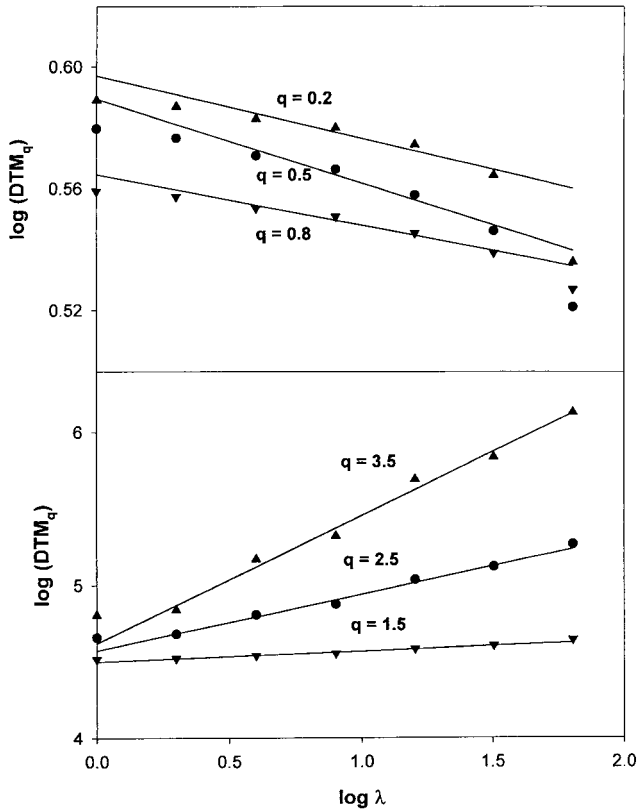


**Figure 8.** Scaling of the moments for various values of  $q$  for the data of Goggin [1998]. In fitting straight lines, the first two points and the last point were not used in the top panel, and the first point was not used in the bottom panel.

work on synthetic multifractal fields). However,  $\sigma$  for Coalinga is almost double  $\sigma$  of Goggin, which indicates that the Coalinga permeability field is more intermittent. The effects of  $\alpha$  and  $\sigma$  are investigated in section 5.

Figure 9 shows plots of the  $M(q)$  functions based on the average  $\alpha$  and  $\sigma$  values reported in Table 1. The agreement between  $M(q)$  obtained based on the UM model and the empirical  $M(q)$  is good in the nonlinear range of the empirical  $M(q)$ . This shows that the UM model is adequate for representing the multifractality of  $K$  at the selected sites.

An important point to consider is the reliability of the parameter estimates. Using synthetically generated UM with 25 independent one-dimensional samples with 1024 points each, Lavallee [1991, p. 80] found that  $\alpha$  could be estimated to an accuracy of approximately  $\pm 0.1$ , which is a rough indication of the enormous sample sizes that are theoretically required. No systematic study on the uncertainty associated with  $\sigma$  and  $H$  has been reported in the literature, but our experience suggests that  $\sigma$  and  $H$  are more accurately estimated than  $\alpha$  [see also Tessier et al., 1993, p. 238]. Nevertheless, one has to be cautious when interpreting the point estimates reported in Table 1, especially for the Coalinga data.

## 5. Generation of Discrete UM Fields

With  $\alpha$ ,  $\sigma$ , and  $H$  known, assume that it is desired to generate a one-dimensional UM field of size  $N$  using a branching ratio  $b = 2$ . This requires that  $N = b^n$ , where  $n$  is the number of cascade steps (note that  $N = \lambda$ ). Following broadly the

approach reported by Wilson et al. [1991] and Pecknold et al. [1993], the following procedure is used:

1. Initially assign a value of 0 over the segment of interest.
2. Split the segment into  $b$  parts and add to each part a Levy noise  $S(\alpha, \beta = -1, \mu = 0, \sigma = 1)$ . Repeat this across each cascade level down to the last level (where  $b^n$  values are obtained).
3. Multiply the values obtained at the last level of step 2 by the constant  $\{\sigma \text{Log } b / (\alpha - 1)\}^{1/\alpha}$  to eventually obtain  $\sigma$  as the codimension of the mean field.
4. Exponentiate the result obtained from step 3.
5. Normalize the field obtained from step 4 by dividing by  $N^{[\sigma/(\alpha-1)]}$ .
6. Fourier transform the field obtained from step 5, and power law filter the transform by multiplying by  $k^{-H}$ , where  $k$  is the wave number.
7. Fourier-transform the field back to physical space to obtain a nonstationary UM field based on the selected values of  $\alpha$ ,  $\sigma$ , and  $H$ .

In dealing with stationary UM, the constant in step 3 above is different from that reported by Wilson et al. [1991] and Pecknold et al. [1993],  $\{\sigma/(\alpha - 1)\}^{1/\alpha}$ , because we included the effect of the branching ratio [e.g., see Gupta and Waymire, 1993]. Furthermore, step 2 was presented because it is less expensive, from a computational point of view, to perform a number of additions and exponentiate at the end than to perform the same number of multiplications.

Using the parameters estimated from the Goggin data as a basis, we illustrate in Figures 13, 14, and 15 the effects of variation in the parameters on simulated UM fields. To facil-

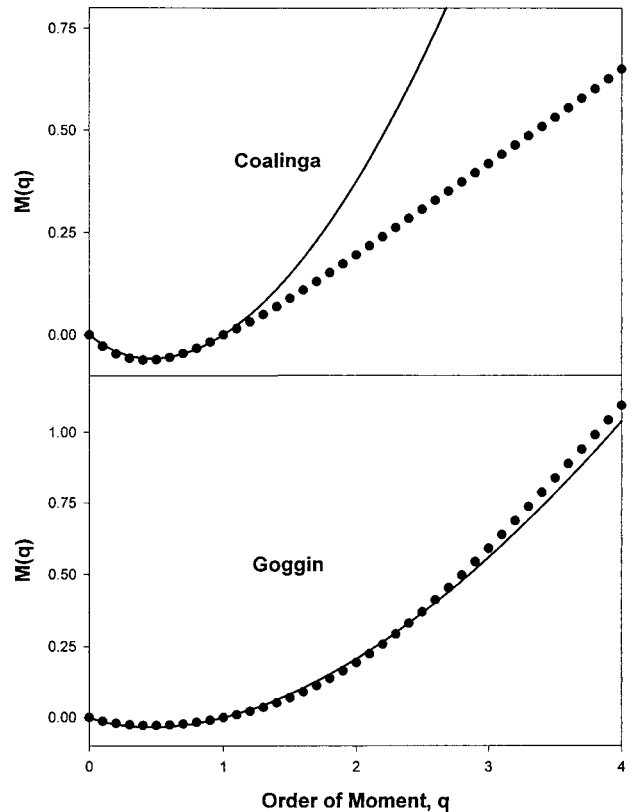
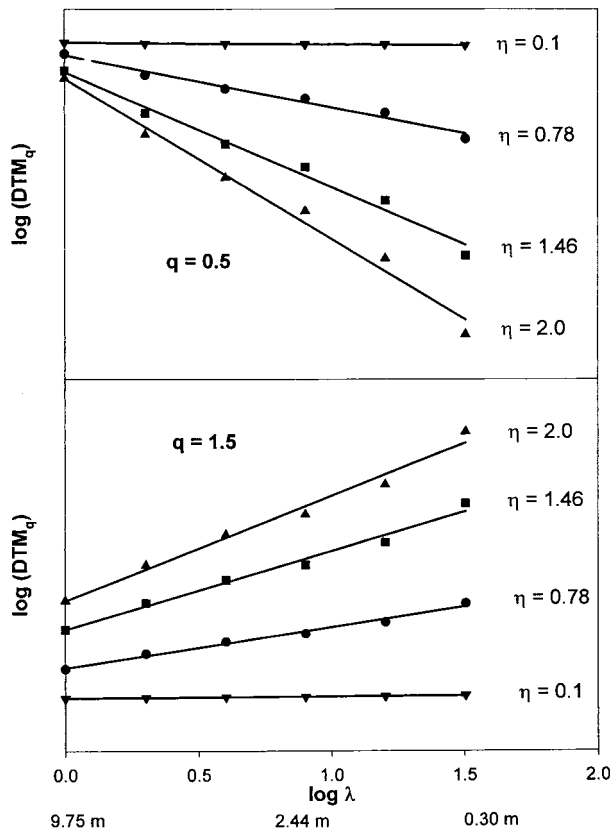


**Figure 9.**  $M(q)$  as a function of  $q$ . The dots represent the empirical  $M(q)$ , and the solid curves represent the one obtained from the universal multifractal model. The nonlinear behavior of  $M(q)$  implies that the  $K$  field is multifractal.

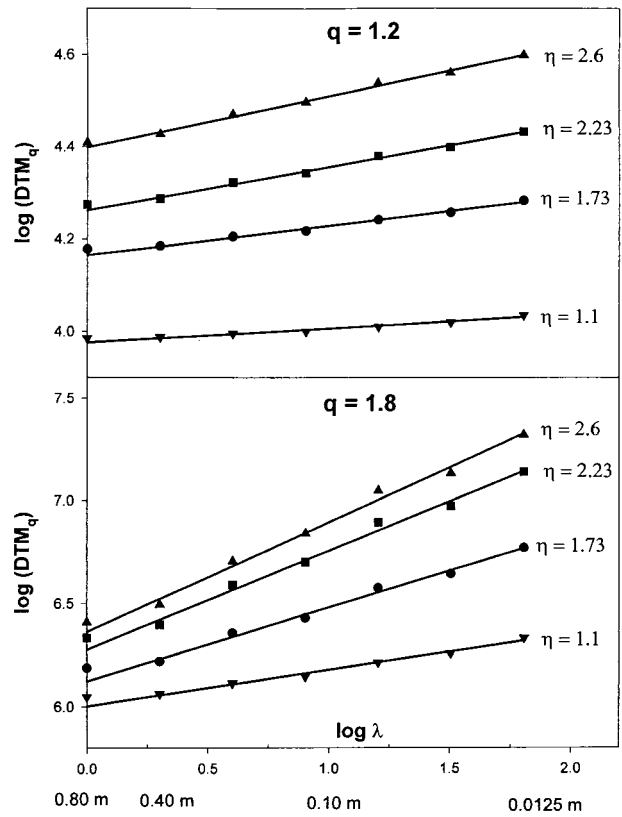
itate visual comparison, we normalized the fields obtained from step 4 above by the mean value of the sample instead of the ensemble mean reported in step 5. Hence all the generated stationary UM fields have a sample mean of 1.0. Each generated field contained  $2^{11} = 2048$  data points, and the seed of the random number generator was the same for all simulations.

Figure 13 shows that the intermittency increases with an increase in  $\sigma$  (note the vertical scale). This is because the (Hausdorff) fractal dimension of the mean value of the field is given by  $D_m = D - \sigma$ , where  $D$  is the topological dimension of the field ( $D = 1$  for a series, such as in this work). From the definition of a fractal dimension,  $D_m$  represents the space-filling ability of the mean field, namely, the ability to fill a (horizontal) threshold line at  $\phi = 1$  (Figure 13). When a field is highly intermittent, such as that in the bottom panel of Figure 13, the mean value of the field is dictated by averaging many very low (near-zero) values and relatively few extreme values. Hence these individual values are far from the mean value of the field. When  $\sigma$  decreases, the low values increase and the maximum values decrease, both approaching the mean value of the field. When  $\sigma$  tends to  $0^+$ ,  $D_m$  tends to fill the whole horizontal line, and hence the low and high values collapse near  $\phi = 1$  and the field becomes essentially uniform (or homogenous).

Figure 14 illustrates the effect of  $\alpha$  on simulated UM stationary fields. Here  $\alpha$  characterizes the rate at which the sparseness of the field varies as we go away from the mean [Tessier *et al.*, 1993, p. 238]. An increase in  $\alpha$  from the base-case value of 1.6 (middle panel of Figure 13) to  $\alpha = 1.9$  did not



**Figure 10.** Scaling of the double trace moment for various values of  $q$  and  $\eta$  for the Coalinga field. Scaling occurs in the linear range.



**Figure 11.** Scaling of the double trace moment for various values of  $q$  and  $\eta$  for the Goggin [1988] data. Scaling occurs in the linear range.

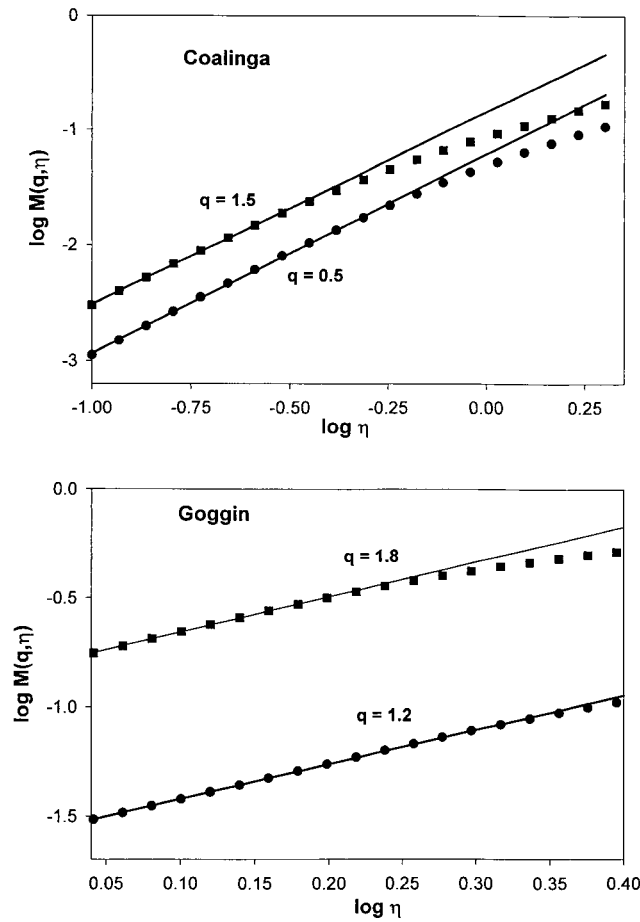
seem to greatly reduce the maximum value of the field, which occurred at a different location from that of the base case. However, at  $\alpha = 1.3$ , the maximum value of the field more than doubled. This is because as  $\alpha$  approaches  $1^+$ , the field becomes so sparse that it does not have a theoretical mean.

Figure 15 shows nonstationary UM for two values of  $H$ . Note that as  $H$  increases from the stationary base case (middle panel of Figure 13), the field becomes smoother because fractional integration induces spatial correlation. Because power law filtering in Fourier space does not apply to wave number  $k = 0$ , the mean value of the field is not much affected (the mean increased by 0.1% in our simulations).

The upper panel of Figure 15 is representative of the Goggin data (Figure 5). It is important to note, however, that visual inspection of generated highly intermittent fields can be deceiving due to their dependence on the seed value used in the random number generator. Furthermore, because the cascade is canonical, one does not expect the statistical properties (i.e.,  $\alpha$  and  $\sigma$ ) to be recovered in every realization [Schertzer and Lovejoy, 1989; Frisch, 1996, p. 148].

## 6. Conclusions

Existing fractal studies dealing with subsurface heterogeneity investigated the scaling and the fractality of the logarithm of the permeability  $K$ . We treated  $K$  as a multifractal and investigated its scaling and fractality using measured horizontal  $K$  data from two locations in the United States. The first data set was from a shoreline sandstone near Coalinga, California, and the second was from eolian sandstone in northern Arizona



**Figure 12.** Plot of  $M(q, \eta)$  as a function of  $\eta$ . The slope of best fit straight lines is equal to  $\alpha$ .

[Goggin, 1988]. By applying spectral analyses and computing the scaling of moments of various orders (using the double trace moment method [Lavalley, 1991; Lavalley et al., 1992, 1993]), we found that  $K$  is multiscaling (i.e., scaling and multifractal). We also found that the so-called universal multifractal (UM) [Schertzer and Lovejoy, 1987] model (essentially log-Levy multifractal) was able to reproduce the multiscaling behavior. The UM model has three parameters: the multifractality index  $\alpha$ , the codimension of the mean field  $\sigma$ , and the “distance” to stationary multifractal  $H$ . We found ( $\alpha = 1.7$ ,  $\sigma = 0.23$ ,  $H = 0.22$ ) and ( $\alpha = 1.6$ ,  $\sigma = 0.11$ ,  $H = 0.075$ ) for the first and second data sets, respectively. The fact that  $\alpha < 2$  implies that the process is non-Gaussian.

Because we dealt with  $K$  directly instead of its logarithm, the intermittency of  $K$  required longer records than previously assumed. The limitation of the data size was an issue in dealing with both data sets; it increased the uncertainty when assessing

**Table 1.** Estimated Values of the Universal Multifractal Model Parameters

Field	Moment	$\alpha$	$\sigma$	$H$
Coalinga	$q = 0.5$	1.73	0.23	0.23
	$q = 1.5$	1.67	0.21	
Goggin	$q = 1.2$	1.62	0.10	0.075
	$q = 1.8$	1.58	0.12	

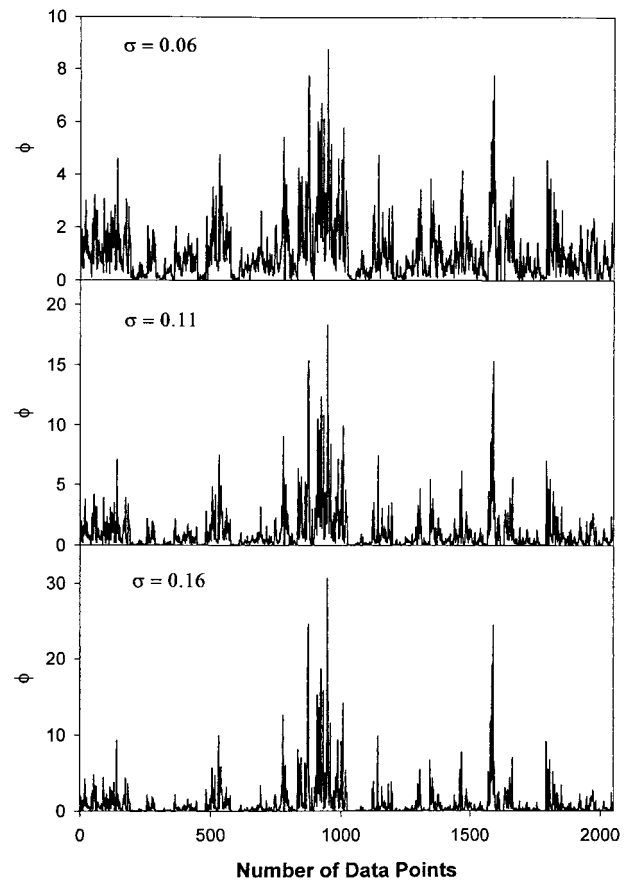


**Figure 13.** Effect of  $\sigma$  on simulated universal multifractal fields;  $\alpha = 1.6$  and  $H = 0.0$ . The field becomes more intermittent when  $\sigma$  increases. The same random seed generator is used here and in Figures 14 and 15.

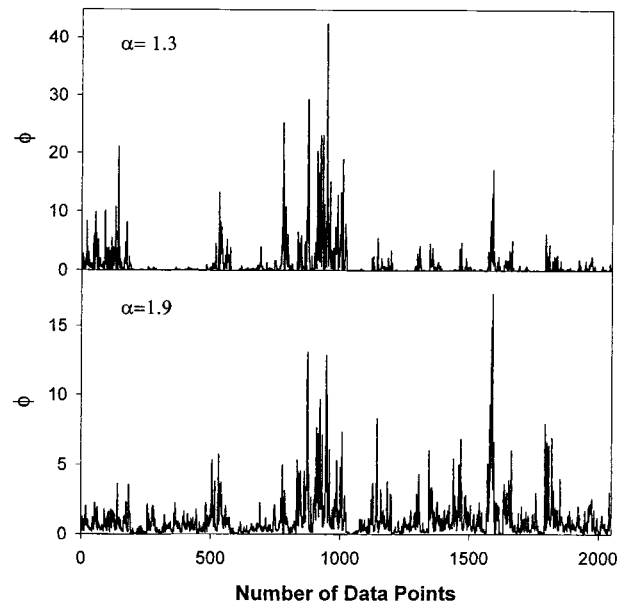


**Figure 14.** Effect of  $\alpha$  on simulated universal multifractal fields;  $\sigma = 0.11$  and  $H = 0.0$ . Compare with the middle panel of Figure 13. The maximum value of the field changes location with a change in  $\alpha$ .

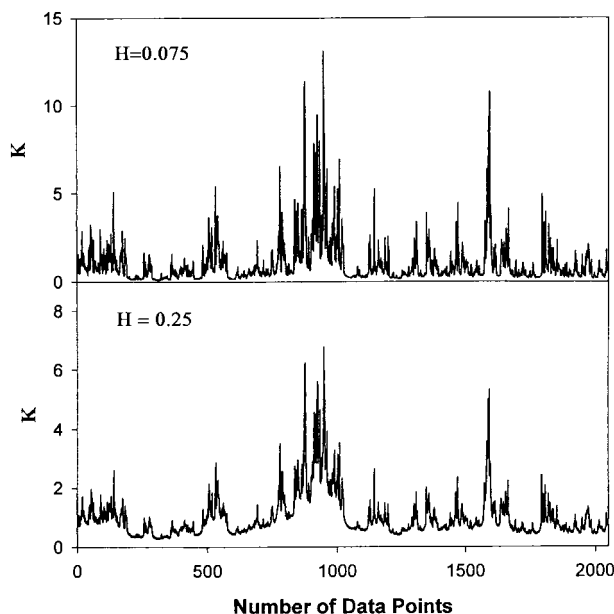


**Figure 15.** Effect of  $H$  on simulated universal multifractal fields;  $\alpha = 1.6$  and  $\sigma = 0.11$ . Compare with the middle panel of Figure 13. The field becomes smoother as  $H$  increases due to an increased spatial correlation.

the multiscaling of the moments and when estimating the UM parameters. It is worth mentioning that even when dealing with the Log  $K$  as the variable of interest, studies by Painter [1996] and Molz *et al.* [1997] suggested the need for larger records when the underlying statistical distribution is Levy-stable.

The ultimate goal of assessing subsurface heterogeneity is for dealing with solute transport. This work investigated the variability of the intrinsic horizontal permeability in the vertical direction. Future work needs to account for anisotropy and the variability in more than one dimension because it is well known that different behaviors of solute plumes occur going from one to three dimensions [Gelhar and Axness, 1983; Attinger *et al.*, 1999].

## Notation

$C(\gamma)$	codimension corresponding to a threshold of order $\gamma$ .
$D$	topological dimension of space.
$H$	“distance” from nonstationary to stationary multifractal.
$M(q)$	moment scaling exponent.
$q$	order of moment.
$Q$	generic variable representing a geophysical multifractal field.
$T$	spectral slope.
$\alpha$	the Levy index and the index of multifractality.
$\beta$	skewness parameter of the Levy distribution.
$\eta$	order of moment used in the double trace moment method.
$\phi$	a stationary multifractal field.
$\gamma$	order of singularity.
$\lambda$	scale ratio ( $\geq 1$ ).
$\mu$	centering parameter of the Levy distribution.

$\sigma$  the scale parameter of the Levy distribution and the codimension of the mean value of a multifractal field.

**Acknowledgments.** This work was funded in part by the U.S. Department of Energy under contract DERA26-97BC15029 and by the National Science Foundation under award 9706048. The authors are grateful to Geoff Pegram and Antony Clothier at the Civil Engineering Department of University of Natal, South Africa, for providing invaluable input regarding the Fourier techniques.

## References

- Attinger, S., M. Dentz, and W. Kinzelbach, Temporal behaviour of a solute cloud in a chemically heterogeneous porous medium, *J. Fluid Mech.*, **386**, 77–86, 1999.
- Brax, P., and R. Peschanski, Levy stable law description of intermittent behaviour and quark-gluon plasma phase transitions, *Phys. Lett. B*, **253**, 225–230, 1991.
- Davis, A., A. Marshak, W. Wiscombe, and R. Cahalan, Multifractal characterizations of nonstationarity and intermittency in geophysical fields: Observed, retrieved, or simulated, *J. Geophys. Res.*, **99**, 8055–8072, 1994a.
- Davis, A., A. Marshak, and W. Wiscombe, Wavelet-based multifractal analysis of non-stationary and/or intermittent geophysical signals, in *Wavelets in Geophysics*, edited by E. Foufoula-Georgiou and P. Kumar, pp. 249–298, Academic, San Diego, Calif., 1994b.
- Davis, A., A. Marshak, W. Wiscombe, and R. Cahalan, Scale invariance of liquid water distributions in marine stratocumulus, part I, Spectral properties and stationary issues, *J. Atmos. Sci.*, **53**, 1538–1558, 1996.
- Feller, W., *An Introduction to Probability Theory and Its Application*, vol. 2, 669 pp., John Wiley, New York, 1971.
- Frisch, U., *Turbulence*, 296 pp., Cambridge Univ. Press, New York, 1996.
- Frisch, U., and G. Parisi, On the singularity structure of fully developed turbulence, in *Turbulence and Predictability in Geophysical Fluid Dynamics*, edited by M. Ghil, R. Benzi, and G. Parisi, pp. 84–88, Elsevier, New York, 1985.
- Frisch, U., P.-L. Sulem, and M. Nelkin, A simple dynamical model of intermittent fully developed turbulence, *J. Fluid Mech.*, **87**, 719–736, 1978.
- Gelhar, L. W., and C. L. Axness, Three-dimensional stochastic analysis of macrodispersion in aquifers, *Water Resour. Res.*, **19**, 161–180, 1983.
- Goggin, D. J., Geologically-sensible modelling of the spatial distribution of permeability in Eolian deposits: Page sandstone (Jurassic), northern Arizona, Ph.D. dissertation, Dep. of Pet. Eng., Univ. of Tex. at Austin, 1988.
- Gupta, V. K., and E. Waymire, Multiscaling properties of spatial rainfall and river flow distribution, *J. Geophys. Res.*, **95**, 1999–2009, 1990.
- Gupta, V. K., and E. Waymire, On lognormality and scaling in spatial rainfall averages, in *Nonlinear Variability in Geophysics*, edited by D. Schertzer and S. Lovejoy, pp. 175–183, Kluwer Acad., Norwell, Mass., 1991.
- Gupta, V. K., and E. Waymire, A statistical analysis of mesoscale rainfall as a random cascade, *J. Appl. Meteorol.*, **32**, 251–267, 1993.
- Halsey, T. C., M. H. Jensen, L. P. Kadanoff, I. Procaccia, and B. I. Shraiman, Fractal measures and their singularities: The characterization of strange sets, *Phys. Rev. A*, **33**, 1141–1151, 1986.
- Hentschel, H. G. E., and I. Procaccia, The infinite number of generalized dimensions of fractals and strange attractors, *Physica D*, **8**, 435–444, 1983.
- Hewett, T. A., Fractal distribution of reservoir heterogeneity and their influence on fluid transport, paper presented at the 61st Annual Technical Conference, Soc. of Pet. Eng., Richardson, Tex., 1986.
- Kida, S., Log-stable distribution and intermittency of turbulence, *J. Phys. Soc. Jpn.*, **60**, 5–8, 1991.
- Kolmogorov, A. N., Local structure of turbulence in an incompressible liquid for very large Reynolds numbers, *Dokl. Acad. Sci. USSR*, **30**, 299–303, 1949.
- Kolmogorov, A. N., A refinement of previous hypotheses concerning the local structure of turbulence in a viscous incompressible fluid at high Reynolds number, *J. Fluid Mech.*, **13**, 82–85, 1962.

- Lavallee, D., Multifractal analysis and simulation technique and turbulent fields, Ph.D. thesis, 133 pp., Dep. of Phys., McGill Univ., Montreal, Que., Canada, 1991.
- Lavallee, D., S. Lovejoy, D. Schertzer, and F. Schmitt, On the determination of universal multifractal parameters in turbulence, in *Topological Aspects of the Dynamics of Fluids and Plasmas*, edited by H. K. Moffat et al., pp. 463–478, Kluwer Acad., Norwell, Mass., 1992.
- Lavallee, D., S. Lovejoy, D. Schertzer, and P. Ladoy, Nonlinear variability and landscape topography: Analysis and simulation, in *Fractals in Geography*, edited by L. De Cola and N. Lam, pp. 158–192, Prentice-Hall, Englewood Cliffs, N. J., 1993.
- Liu, H. H., and F. J. Molz, Multifractal analyses of hydraulic conductivity distributions, *Water Resour. Res.*, **33**, 2483–2488, 1997.
- Lovejoy, S., D. Lavallee, D. Schertzer, and P. Ladoy, The  $1^{1/2}$  law and multifractal topography: Theory and analysis, *Nonlinear Processes Geophys.*, **2**, 16–22, 1995.
- Mandelbrot, B. B., Intermittent turbulence in self-similar cascades: Divergence of high moments and dimension of the carrier, *J. Fluid Mech.*, **62**, 331–358, 1974.
- Mandelbrot, B. B., *The Fractal Geometry of Nature*, 460 pp., W. H. Freeman, New York, 1982.
- Meneveau, C., and K. R. Sreenivasan, The multifractal spectrum of the dissipation field in turbulent flows, *Nucl. Phys. B Proc. Suppl.*, **2**, 49–76, 1987a.
- Meneveau, C., and K. R. Sreenivasan, Simple multifractal cascade model for fully developed turbulence, *Phys. Rev. Lett.*, **59**, 1424–1427, 1987b.
- Molz, F. J., and G. Boman, A fractal-based stochastic interpolation scheme in subsurface hydrology, *Water Resour. Res.*, **29**, 3769–3774, 1993.
- Molz, F. J., and G. Boman, Further evidence of fractal structure in hydraulic conductivity distributions, *Geophys. Res. Lett.*, **22**, 2545–2548, 1995.
- Molz, F. J., H. H. Liu, and J. Szulga, Fractional Brownian motion and fractional Gaussian noise in subsurface hydrology: A review, presentation of fundamental properties, and extensions, *Water Resour. Res.*, **33**, 2273–2286, 1997.
- Monin, A. S., and A. M. Yaglom, *Statistical Fluid Mechanics: Mechanics of Turbulence*, edited by J. L. Lumley, 874 pp., MIT Press, Cambridge, Mass., 1975.
- Obukhov, A., Some specific features of atmospheric turbulence, *J. Geophys. Res.*, **67**, 3011–3014, 1962.
- Painter, S., Evidence for non-Gaussian scaling behavior in heterogeneous sedimentary formations, *Water Resour. Res.*, **32**, 1183–1195, 1996.
- Painter, S., Numerical methods for conditional simulation of Levy random fields, *Math. Geol.*, **30**, 163–179, 1998.
- Painter, S., and G. Mahinthakumar, Prediction uncertainty for tracer migration in random heterogeneities with multifractal character, *Adv. Water Resour.*, **23**, 49–57, 1999.
- Painter, S., and L. Paterson, Fractional Levy motion as a model for spatial variability in sedimentary rock, *Geophys. Res. Lett.*, **21**, 2857–2860, 1994.
- Pecknold, S., S. Lovejoy, D. Schertzer, C. Hooge, and J. F. Malouin, The simulation of universal multifractals, in *Prospects in Astronomy and Astrophysics*, edited by J. M. Perdand and A. Lejeune, pp. 228–267, World Sci., River Edge, N. J., 1993.
- Peitgen, H.-O., and D. Saupe (Eds.), *The Sciences of Fractal Images*, 312 pp., Springer-Verlag, New York, 1988.
- Samorodnitsky, G., and M. S. Taqqu, *Stable Non-Gaussian Random Processes*, 632 pp., Chapman and Hall, New York, 1994.
- Schertzer, D., and S. Lovejoy, Physical modeling and analysis of rain and clouds by anisotropic scaling multiplicative processes, *J. Geophys. Res.*, **92**, 9693–9714, 1987.
- Schertzer, D., and S. Lovejoy, Nonlinear variability in geophysics: Multifractal simulations and analysis, in *Fractals: Physical Origin and Properties*, edited by L. Pietronero, pp. 49–79, Plenum, New York, 1989.
- Schertzer, D., S. Lovejoy, D. Lavallee, and F. Schmitt, Universal hard multifractal turbulence: Theory and observations, in *Nonlinear Dynamics of Structures*, edited by R. Z. Sagdeev et al., pp. 213–235, North-Holland, New York, 1991.
- Schmitt, F., S. Lovejoy, and D. Schertzer, Multifractal analysis of the Greenland Ice Core Project climate data, *Geophys. Res. Lett.*, **22**, 1689–1692, 1995.
- Tatom, F. B., The relationship between fractional calculus and fractals, *Fractals*, **3**, 217–229, 1995.
- Tessier, Y., S. Lovejoy, and D. Schertzer, Universal multifractals: Theory and observations for rain and clouds, *J. Appl. Meteorol.*, **32**, 223–250, 1993.
- Veneziano, D., Basic properties and characterization of stochastically self-similar processes in  $R^d$ , *Fractals*, **7**, 59–78, 1999.
- Waymire, E., Scaling limits and self-similarity in precipitation fields, *Water Resour. Res.*, **21**, 1271–1281, 1985.
- Wilson, J., D. Schertzer, and S. Lovejoy, Continuous multiplicative cascade models of rain and clouds, in *Nonlinear Variability in Geophysics*, edited by D. Schertzer and S. Lovejoy, pp. 185–207, Kluwer Acad., Norwell, Mass., 1991.
- Yaglom, A. M., The influence of the fluctuation in energy dissipation on the shape of turbulent characteristics in the inertial interval (in Russian), *Sov. Phys. Dokl.*, **2**, 26–30, 1966.

M. C. Boufadel, Department of Civil and Environmental Engineering, Temple University, 1947 North 12th Street, Philadelphia, PA 19122. (boufadel@astro.temple.edu)

D. Lavallee, Institute for Crustal Studies, University of California, Santa Barbara, Santa Barbara, CA 93106.

S. Lu and F. J. Molz, Environmental Engineering and Science Department, Clemson University, Clemson, SC 29631.

(Received March 20, 2000; revised June 12, 2000; accepted July 5, 2000.)